研究論文

Size of Elementary Clusters in Silver Nanoparticle Formation

銀ナノ粒子形成過程における素クラスターサイズ

Masafumi TAKESUE*[1] 武居　正史
Takuya TOMURA*[1] 外村　卓也
Mitsuru YAMADA*[1] 山田　充
Katsuhiko HATA*[1] 畑　克彦
Shigeo KUWAMOTO*[2] 桑本　滋生
Tetsu YONEZAWA*[3] 米澤　徹

銀ナノ粒子形成過程における素クラスターサイズを明らかにするために、高輝度放射光を用いた小角X線散乱測定を行った。既往の研究より3オーダー高精度な0.18ミリ秒の時間分解能で測定可能な専用の反応器を設計し、クラスターサイズの変化をその場観察で追跡した。その結果、銀ナノ粒子はAg_{13}クラスターに相当する0.7nmサイズのクラスターを介して形成されていることがわかった。

1. Introduction

Silver and gold metal nanoparticles can be sintered on polymer films [1-4] and even paper [5] due to melting point depression and size effects [1,2,4,6], and thus have attracted much attention in electro-conductive metallic inks for printed electronics [2,4,7,8]. Practical applications would require specific particle size distributions to enable fabrication of closely-packed layers of nanoparticles rather than monodispersed nanoparticles [1,4]. Therefore, a better understanding of the formation mechanism of noble metal nanoparticles is needed to prepare desired diameter and size distribution formulations. Classical growth models state that particles are formed by means of monomer addition after a discrete nucleation period [9], while recent studies show that silver and gold nanoparticles are formed via a complex pathway including a broad nucleation period with simultaneous particle growth period [10-14]. Generally, it can be considered that a cluster consisting of several atoms rather than a single atom acts as an elementary species that determine monomer addition and particle growth. Silver and gold metal clusters along with the full-shell clusters, in which a central atom is surrounded by shells of atoms to form an icosahedron, are thought to be thermodynamically stable [15], and the cluster sizes of the first- and second-full-shell clusters, Ag_{13} and Ag_{55} are estimated to be 0.7 and 1.2 nm [16,17], respectively. The existence of the Ag_{13} cluster, however, has not been clarified in previous literature unlike Au_{13} clusters [15,18], although its attractive magnetic properties have been widely discussed with the help of computational science [19].

Small angle X-ray scattering (SAXS) could be an effective technique to evaluate *in situ* size distribution of nanoparticles, because it has the potential to statistically process a very large number of particles [12,20-22]. Previous studies, however, have not clearly established the size of elementary silver clusters, because the determination of this size would require *in situ* observation at an extremely high time resolution (*ca*. a few ms). Detailed discussion of the formation mechanism with SAXS would also require a specialized apparatus rather than under batch-type conditions to completely fix the onset of the formation of all particles. In this work, we have used a custom-fabricated one-direction-of-flow reactor cell to obtain *in situ* SAXS curves at high time resolutions of 0.18 ms, which is three orders of magnitude higher than those used in previous studies (*ca*. 100 ms) [12,20]. By analyzing the time dependence of SAXS curves *in situ* for silver nitrate solutions that are reacted with reducing solutions containing trisodium citrate [23,24] as a weak dispersant, we discuss fine details of the sizes of the elementary clusters forming and the mechanism of silver nanoparticles formation in aqueous system.

2. Experimental

Conventional chemical reduction in an aqueous system was used for the examination of the formation of silver

---

*[1] R&Dセンター
*[2] ひょうご科学技術協会
*[3] 北海道大学

nanoparticles. A one-direction-of-flow reactor cell, made of poly (methyl methacrylate) resin equipped with thin polyimide film windows and with two injection flow channels enabled mixing of two influent solutions and a single efficient flow channel. Silver ion solution was mixed with a reducing solution and fed at equal flow rates, 120 mL min^{-1}, into a mixing point to allow mixing under turbulent flow conditions. The SAXS measurements were carried out at the BL08B2 beamline in SPring-8 synchrotron radiation facility in Japan. The reactor cell was set on a vertically movable stage to control the X-ray irradiation position axially from the mixing point. For the mixing point defined as the point of origin, 0 ms reaction time, a distance of1mm along the reactor cell corresponded to a reaction time of 0.393 ms based on the given flow rate. A maximum time resolution of 0.18 ms was possible for a vertical beam size of 0.23 mm. The two-dimensional scattering images detected on the X-ray imaging plate were converted to one-dimensional scattering curves giving the scattering vector (q) dependence of scattering intensities by azimuthal integration and subtraction of each scattering curve of the solution including all chemicals except for the silver ions. The size distribution of the silver nanoparticles and clusters was determined by curve fitting with a gamma distribution function [25].

3. Results and discussion

The time dependence of the scattering intensities of the SAXS curves, that of the particle size distributions fitted with the intensities, and analysis of the time dependence of the nanoparticles and clusters are shown in Figure 1. The drop in the scattering intensities at q lower than around 0.025 Å^{-1} in all curves (Figure 1a) was due to shielding of the beam stopper, so these areas can be excluded from discussion.

The scattering curves were almost flat and constant at reaction times of 0 and 0.39 ms. This means that the q ranges may not reach the Porod region because particles are too small or absent at the given reaction times. Curve fittings at short reaction times of 0 and 0.39 ms had high uncertainties and are not displayed. In the induction period, the reduction process from Ag$^+$ ions to Ag^0 atoms are most likely taking place, but the nucleation has not been initiated. Still, even at this high time resolution, it was not possible to describe the progress of the reduction process completely with the SAXS measurements.

The scattering curves appeared distinct rising in the slopeover 0.59 ms. Curves at reaction times greater than 0.59 ms could be well fitted throughout the whole q range. It is probable that there is a trigger for the onset of nucleation of silver clusters and nanoparticles between the 0.39 and 0.59 ms, and the onset becomes clear at 0.59 ms.

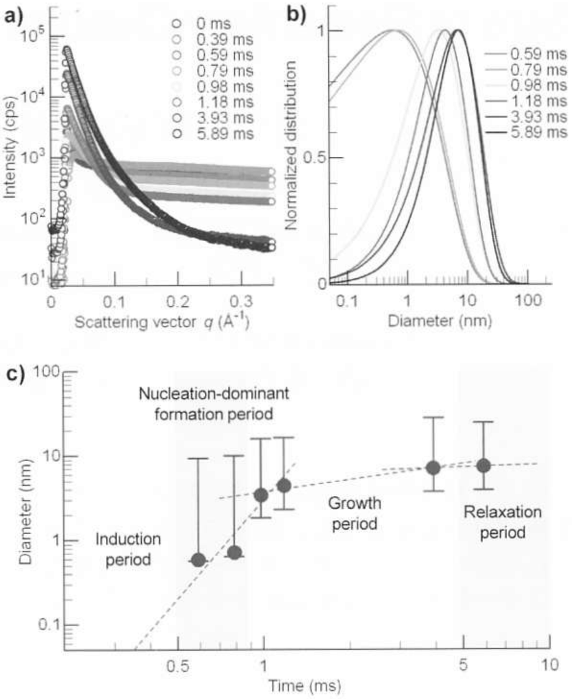

Figure 1. Time dependence of silver clusters and nanoparticles formation. a) Small angle X-ray scattering (SAXS) curves measured in the custom-fabricated one-direction-of-flow reactor cell. b) Particle size distribution fitted with the SAXS curves. c) Time dependence of peak diameter (solid circles) and the particle diameters at volume fractions of 10% and 90% (error bars). Proposed periods of silver nanoparticle formation process are overlaid. Dashed lines show power approximation fits to help distinguish growth rate periods.

At 0.59 and 0.79 ms reaction times, when nucleation had started according to the increase in the particle sizes, the peak diameters were 0.58 and 0.71 nm, respectively, indicating that the nucleation of Ag_{13} clusters corresponding to 0.7nm in diameter predominated at the 0.59 and 0.79 ms reaction times. On the other hand, the observed larger diameters in the size distributions at 0.59 and 0.79 ms, namely, over 10nm, are evidence that the growth of silver nanoparticles had started along with the nucleation. This nucleation-dominant formation period, in which Ag_{13} clusters were nucleated and consumed in the simultaneous formation and growth of silver nanoparticles, was almost certainly not continuing at 0.98 ms, as shown by volume fractions that were approximate 0.7 nm in size and considerably decreasing with reaction time. Although the limited experiments performed in this study prevent quantitative discussion on whether all silver atoms went through Ag_{13} clusters, the particle size distributions show that Ag_{13} clusters are the dominant species during the nucleation-dominant formation period.

The distinct change in the particle size distributions appeared as abrupt increases of the peak diameters at and later than the reaction time of 0.98 ms. The peak diameters of the silver nanoparticles increased from 0.71 to 3.36 nm at reaction times between 0.79 and 0.98 ms, and the 10%volume fraction of particles was 1.82 nm at 0.98 ms, suggesting that Ag_{13} clusters were depleted at 0.98 ms. The nucleation of Ag_{13} clusters seemed to be complete terminated at 0.98 ms, and the growth of silver nanoparticles predominated after 0.98 ms. The main process in this growth period is most likely coalescence among smaller silver nanoparticles, which were formed mainly by agglomeration of Ag_{13} clusters during the previous nucleation-dominant formation period. Alternatively, there is the possibility that silver nanoparticles grew continuously by the addition of silver atoms reduced in the early period on Ag_{13} clusters. In that case, silver nanoparticle formation would grow via Ag_{55} clusters, which are the next full-shell clusters and 1.2 nm in diameter. However, the fraction of particles having diameters of around 1.2 nm was not dominant during a period between 0.79 and 0.98 ms. Although it is not possible to completely ignore the possible presence and contribution of Ag_{55} clusters in the particle formation process since a small volume fraction of particles around 1.2 nm in diameter does exist, the silver atoms reduced can be assumed to preferentially take part in the immediate nucleation of Ag_{13} clusters rather than remaining as is for an extended period awaiting consumption in the formation of Ag_{55} clusters. Therefore, it can be hypothesized that silver nanoparticles grow mainly via Ag_{13} clusters rather than clusters in other sizes. Namely, Ag_{13} clusters play an important role as an elementary cluster in the formation of the silver nanoparticles.

The peak diameters gradually increased from 3.36 nm at 0.98 ms to 6.95 nm at 3.93 ms, where larger particles were over 20 nm in diameter, and at the reaction time of 5.89 ms, the peak diameters showed only a slight increase (Figure 1 c).This means that the growth process was substantially complete at 3.93 ms. At 3.93 and 5.89 ms, 90% of the volume fraction was over 3 nm. Particle growth is terminated by the consumption of silver nanoparticles smaller than around 3 nm in diameter, which have relatively high surface activity. The particle size distribution narrowed slightly at 5.89 ms, compared with that at 3.93 ms, which may be attributed to a relaxation or rearrangement of transient aggregated larger particles during this relaxation period after 3.93 ms, and not to a recrystallization of smaller particles by "size distribution focusing" [11] or Ostwald ripening [13,14], because the process occurred during a short duration of around 2 ms. Further elucidation of the relaxation process requires additional experiments and a greater number of data.

The formation of silver nanoparticles, which were formed in an aqueous system, proceeded during a very short reaction time of around 6 ms and seemed to consist of four distinct periods as proposed in Figure 1c and shown schematically as a formation mechanism in Figure 2. After a short induction period, in which silver ions are reduced, Ag_{13} clusters are actively formed, and subsequently small silver nanoparticles are formed mainly by agglomeration among Ag_{13} clusters (nucleation-dominant formation period). The formation of silver nanoparticles seemed to have no discrete nucleation period according to the time-scales and methods used in this work. The Ag_{13} clusters were practically consumed during the nucleation-dominant formation period. Particle growth occurs by coalescence and aggregation among the small silver nanoparticles resulting in larger silver nanoparticles (growth period). Finally, the growth stage is complete with the consumption of all small silver nanoparticles, and as a final process, the transient aggregated particles relax to increase the particle size slightly. In this stage, the particle size distribution narrows (relaxation period).

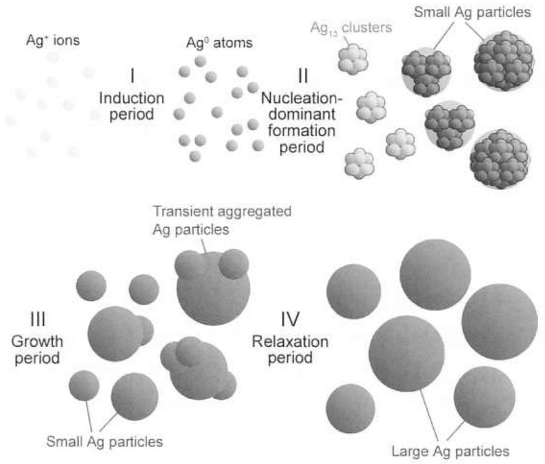

Figure 2. Proposed formation mechanism of silver nanoparticles via Ag_{13} clusters. Silver nanoparticles are formed through: I) Induction period, in which Ag^+ ions were reduced to Ag^0 atoms; II) Nucleation-dominant formation period, in which Ag_{13} clusters are nucleated and simultaneously consumed for Ag nanoparticle formation; III) Growth period, in which larger Ag nanoparticles are formed by coalescence and aggregation among smaller Ag nanoparticles; IV) Relaxation period, in which particle size distribution slightly narrows by relaxation or rearrangement of transient aggregated particles.

4. Conclusion

The formation of silver nanoparticles has no discrete nucleation period according to the time-scale and methods used in this work. The SAXS results here show that silver nanoparticles are formed via four distinct periods within 6 ms, and that the diameter of the silver nanoparticles increases mainly via an approximately 0.7 nm cluster corresponding to the size of a Ag_{13} cluster. Ag_{13} clusters play an important role as an elementary cluster in the formation of silver nanoparticles.

Acknowledgement

This study has been carried out through CREATE organized by Hyogo Prefecture funded by JST for development of common ground of nanoparticle composite. We thank Prof. Emeritus Katsuhiko Nakamae (Kobe Univ.) for pushing this study forward, Masanori Kiyoi (Bando Chemical) for designing the feeding apparatus, and Prof. Richard L. Smith Jr. (Tohoku Univ.) for many valuable discussions. TY thanks the partial financial support from Grant-in-Aid for Scientific Research (B) (21310072) from JSPS and Grant-in-Aid for Scientific Research in Priority Area (Strong Photon-Molecule Coupling Fields for Chemical Reactions (470,21020010) from MEXT, Japan.

References

[1] Moon, K.-S.; Dong, H.; Maric, R.; Pothukuchi, S.; Hunt, A.; Li, Y.; Wong, C. P. *J. Electronic Mater*. **2005**, *34*, 168-175.

[2] Sivaramakrishnan, S.; Chia, P.-J.; Yeo, Y.-C.; Chua, L.-L.; Ho, P. K.-H. *Nature Mater*. **2007**, *6*, 149-155.

[3] Klajn, R.; Bishop, K. J. M.; Fialkowski, M.; Paszewski, M.; Campbell, C. J.; Gray, T. P.; Grzybowski, B. A. *Science* **2007**, *316*, 261-264.

[4] Perelaer, J.; Hendriks, C. E.; de Laat, A. W. M.; Schubert, U. S. *Nanotechnology* **2009**, *20*, 165303.

[5] Magdassi, S.; Grouchko, M.; Berezin, O.; Kamyshny, A. *ACS Nano* **2010**, *4*, 1943-1948.

[6] Tao, A.; Sinsermsuksakul, P.; Yang, P. *Nature Nanotech*. **2007**, *2*, 435-440.

[7] Shimoda, T.; Matsuki, Y.; Furusawa, M.; Aoki, T.; Yudasaka, I.; Tanaka, H.; Iwasawa, H.; Wang, D.; Miyasaka, M.; Takeuchi, Y. *Nature* **2006**, *440*, 783-786.

[8] Rogers, J. A.; Someya, T.; Huang, Y. *Science* **2010**, *327*, 1603-1607.

[9] LaMer, V. K.; Dinegar, R. H. *J. Am. Chem. Soc*.**1950**, *72*, 4847-4854.

[10] Biswas, K.; Varghese, N.; Rao, C. N. R. *Small* **2008**, *4*, 649-655.

[11] Zheng, H.; Smith, R. K.; Jun, Y.-W.; Kisielowski, C.; Dahmen, U.; Alivisatos, A. P. *Science* **2009**, *324*, 1309-1312.

[12] Polte, J.; Erler, R.; Thünemann, A. F.; Sokolov, S.; Ahner, T. T.; Rademann, K.; Emmerling, F.; Kraehnert, R. *ACS Nano* **2010**, *4*, 1076-1082.

[13] Richards, V. N.; Rath, N. P.; Buhro, W. E. *Chem. Mater*. **2010**, *22*, 3556-3567.

[14] Meli, L.; Green, P. F. *ACS Nano* **2008**, *2*, 1305-1312.

[15] Schmid, G. *Chem. Soc. Rev*. **2008**, *37*, 1909-1930.

[16] Amano, C.; Niina, H.; Mikami, Y. *Theochem*. **2009**, *904*, 64-68.

[17] Harb, M.; Rabilloud, F.; Simon, D. *Phys. Chem. Chem. Phys*. **2010**, *12*, 4246-4254.

[18] Shichibu, Y.; Konishi, K. *Small* **2010**, *6*, 1216-1220.

[19] Piotrowski, M. J.; Piquini, P. *Phys. Rev. B* **2010**, *81*, 155446.

[20] Abécassis, B.; Testard, F.; Spalla, O. *Phys. Rev. Lett*. **2008**, *100*, 115504.

[21] Lee, G.-W.; Jin, K. S.; Kim, J.; Bae, J.-S.; Yeum, J. H.; Ree, M.; Oh, W. *Appl. Phys. A* **2008**, *91*, 657-661.

[22] Plech, A.; Kotaidis, V.; Siems, A.; Sztucki, M. *Phys. Chem. Chem. Phys*. **2008**, *10*, 3888-3894.

[23] Chen, H. M.; Hsin, C. F.; Liu, R.-S.; Lee, J.-F.; Jang, L.-Y. *J. Phys. Chem. C* **2007**, *111*, 5909-5914.

[24] Mpourmpakis, G.; Vlachos, D. G. *Phys. Rew. Lett*. **2009**, *102*, 155505.

[25] Yao, H.; Miki, K.; Nishida, N.; Sasaki, A.; Kimura, K. *J. Am. Chem. Soc*. **2005**, *127*, 15536-15543.

〔付　記〕

Adapted with permission from *Journal of the American Chemical Society* **2011**, *133*, 14164-14167. Copyright 2011 American Chemical Society.

武居　正史
Masafumi TAKESUE
1990年入社
R&D センター

外村　卓也
Takuya TOMURA
1999年入社
R&D センター

山田　充
Mitsuru YAMADA
2005年入社
R&D センター

畑　克彦
Katsuhiko HATA
1985年入社
R&D センター